Available online at www.sciencedirect.com
SCIENCE DIRECT®
International Journal of Thermal Sciences 42 (2003) 15–22
International Journal of Thermal Sciences
www.elsevier.com/locate/ijts

Modeling of flow and thermo-kinetics during the cure of thick laminated composites ☆

V.A.F. Costa [a], A.C.M. Sousa [b,*]

[a] *Department of Mechanical Engineering, University of Aveiro, 3810.193 Aveiro, Portugal*
[b] *Department of Mechanical Engineering, University of New Brunswick, Fredericton, NB, Canada E3B 5A3*

Received 8 May 2001; accepted 3 January 2002

Abstract

The present work describes a three-dimensional numerical model developed to simulate and to analyse the mechanisms dealing with resin flow, heat transfer and the cure of thick composite laminates during autoclave processing. The model, which incorporates some of the best features of models already reported in the literature, is based on the Darcy law, the convection-diffusion heat equation, and appropriate constitutive relations. The model's predictions show that the final degree of consolidation is strongly dependent upon the compacting pressure, which corroborates previous work, and, to a great extent, upon the edge bleeding flow—a finding, which had not been clearly identified before in the literature. The simulations were conducted using the parameters that describe the resin kinetics and rheological behavior of Hercules ASA/3501-6 tape, however, the model is general enough to accommodate different types of tape. The predictions are in good agreement with the results available in the literature, notwithstanding a few concerns related to the final consolidation level of the composite.

1. Introduction

The fabrication of a large number of advanced polymer composites has been relying upon the autoclave-assisted cure of prepregs, i.e., resin preimpregnated fibers. To form the laminate of desired thickness it is required that prepregs be placed on a smooth tool surface in a predetermined fiber orientation for each layer (Fig. 1). Also, an absorbent material, the bleeder, is usually placed on both sides of the composite. To facilitate the removal of the composite after processing, a sheet of nonporous teflon release cloth is placed between the composite and the tool, and a sheet of porous teflon release cloth is placed between the composite and the bleeder. A metal lid covers the bleeder, and an air breather is placed on top of the lid. The so-called "dams" are mounted to restrict lateral motion and to control the resin flow through the edges. A plastic cover—the vacuum bag, encloses the complete assembly. During the cure, vacuum is applied to the assembly, which is exposed to properly controlled temperature and pressure cycles to guarantee that the laminates be fully compacted and well cured. For thick laminates, the understanding of the occurring consolidation and curing processes is critical to guide the composite manufacturing prerequisites.

The chemical reaction is exothermic, and for thick laminates, which can be several centimeters thick, there is a strong possibility of "hot spots", which may yield uneven resin distribution. This process strongly depends upon the simultaneous interplay of the chemical reaction, heat transfer and resin flow. As stated in [1], the resin flow is the primary mechanism for removing excess resin, eliminating voids inside the laminate, and achieving the desired fiber volume fraction. The control of this flow, however, is not trivial, because the flow itself is a function of the temperature, and reaction kinetics. The control of temperature in the core region poses a difficult problem, in particular for thick laminates. The combined effect of low thermal conductivity and large thickness yields temperatures in the core region lower than those experienced by the material edges, causing limited flow in the core region as a result of the higher viscosity. Beyond a certain temperature threshold, however, the temperature rises due to the reaction exotherm, and material degradation, if the reaction is out of control, is an ever-

☆ An earlier version of this paper was presented at IDMME'2000, Forum 2000, SCGM/CSME, Montreal, Quebec, Canada.

* Correspondence and reprints.
E-mail address: asousa@unb.ca (A.C.M. Sousa).

1290-0729/02/$ – see front matter
PII: S1290-0729(02)00003-0

Nomenclature

A_1, A_2, A_3	experimental parameters	min^{-1}	
B, C	factors of the conductivity model		
c	combined specific heat of resin and fibers	$\text{kJ·kg}^{-1}\text{·K}^{-1}$	
c_r	specific heat of the resin	$\text{kJ·kg}^{-1}\text{·K}^{-1}$	
e	ratio between the volume of resin and the volume of fibers (void ratio)		
k_f	thermal conductivity of the fibers	$\text{W·m}^{-1}\text{·K}^{-1}$	
k_r	thermal conductivity of the resin	$\text{W·m}^{-1}\text{·K}^{-1}$	
k_{xx}, k_{yy}, k_{zz}	combined thermal conductivities of resin and fibers in the x-, y-, and z-direction, respectively	$\text{W·m}^{-1}\text{·K}^{-1}$	
K	constant of the rheological model		
K_1, K_2, K_3	kinetics parameters	s^{-1}	
K_{xx}	Kozeny constant (0.7)		
K_{zz}	model constant		
m_v	coefficient of volume compressibility	Pa^{-1}	
$\dot{m}'''$	mass conversion rate	$\text{kg·s}^{-1}\text{·m}^{-3}$	
p_f	pressure sustained by the fibers	Pa	
p_r	pressure of the resin	Pa	
r_f	fiber radius	m	
R	universal gas constant	$\text{J·K}^{-1}\text{·mol}^{-1}$	
S_{ij}	permeabilities	m^2	
T	temperature	K	
T_0	cure temperature	K	
u, v, w	velocity components in the x-, y-, and z-direction, respectively	m·s^{-1}	
U	parameter of the rheological model	J·mol^{-1}	
V_f	fiber volume fraction		
V_r	resin volume fraction		
V'_a	"shut off" volume fraction		
V'_f	volume of the fibers	m^3	
V'_r	volume of the resin	m^3	
x, y, z	Cartesian coordinates	m	

Greek symbols

α	resin conversion	
$\Delta E_1, \Delta E_2, \Delta E_3$	activation energies	J·mol^{-1}
ΔH	heat of reaction per unit mass of resin	kJ·kg^{-1}
μ	viscosity	$\text{kg·s}^{-1}\text{·m}^{-1}$
μ_∞	parameter of the rheological model	Pa·s
ρ	combined density of resin and fibers	kg·m^{-3}
ρ_r	density of the resin	kg·m^{-3}
σ	applied pressure	Pa

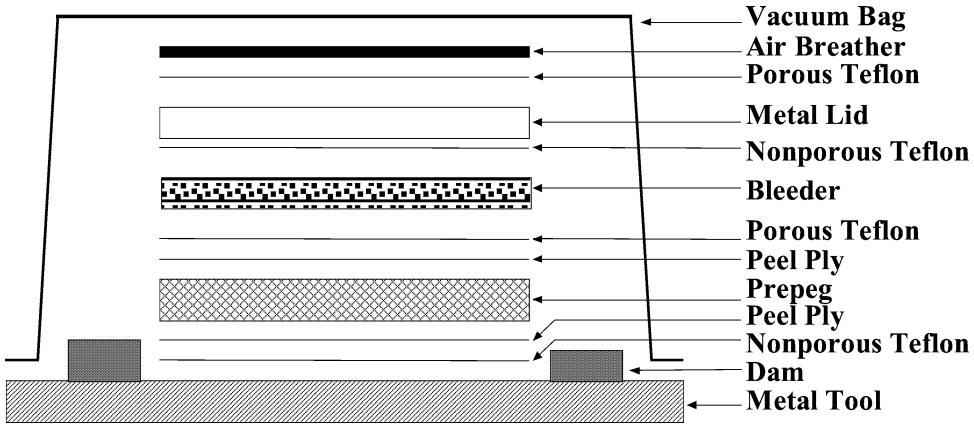

Fig. 1. Vertical "exploded" view of a composite lay-up.

present possibility. In addition, high temperature gradients across the thickness of the laminate may yield poor quality material due to different levels of cure, and high thermal stresses.

The driving force toward the development of a comprehensive, reliable numerical model lies in its potential contribution to the manufacturing process. A well-tested and well-benchmarked model may help to expedite the formulation of an appropriate cure cycle for a particular material.

The paper presents a brief review of selected modeling work [1–14] conducted to analyze the consolidation and cure of composites. In addition, this paper presents a numerical model, which permits to extend the analyses presented in [1]. The present model takes into consideration the compacting forces and their effects upon the variation of thickness, porosity, fiber permeability, and thermal properties. The three-dimensional governing equations for resin flow and heat transfer are fully described along with compatible constitutive relations. The set of equations is solved using a finite volume procedure developed for unstructured meshes, which has the advantage of coping well with the solution of the elastic stress-strain equations, which, however, are not part of the present study.

2. Modeling—A brief review

The baseline for a numerical model was well described in [2]. A model should be capable of providing information on temperature, pressure, degree of cure of the resin, and resin viscosity, in terms of their spatial distribution within the composite and time development. In addition, it is important to know as a function of time: number of compacted prepeg plies, amount of resin in the bleeder, and the thickness of the composite. Ultimately, it will be required to have the capability of predicting void sizes and location, and the time development of the pressure and temperature inside the voids, and after cure, the residual stresses.

The review will be conducted under three subheadings, which, to a great extent, correspond to different components of the numerical model. The subheadings are configuration, flow, and thermo-kinetics. The model also includes the "voids", and "stresses" submodels, but since they are not relevant to the present work, they will not be discussed here.

2.1. Configuration

The system to be modeled only considers the prepegs and the bleeder—this one in its contribution to pressure at the laminate edges, as the other components—vacuum bag, air breather, teflon sheets, peel plies, and lid, play no significant role upon the behavior of the variables of interest.

At a particular instant of time the system is exposed to a convective/radiative environment of known temperature, T_0, which is assumed to be the cure temperature and it is simultaneously subjected to a pressure, σ. The cure temperature, T_0, and the pressure, σ, may vary with time in any pre-specified desired fashion. The resin may flow in the direction normal and parallel to the plane of the prepeg. The consolidation process is assumed to be one-dimensional in the direction of the force resulting from the applied pressure, σ.

2.2. Flow

The pressure applied to the composite yields the resin flow along the fibers and in the direction normal to the fibers. Early research work in the modeling of the resin flow incorporated considerable simplifying assumptions. For instance, in [3] is presented one of the earliest models for the flow, where it is recognized that the squeezing flow mechanism provides the only driving force of the flow within the laminates. The model is largely based on a one-dimensional momentum equation based on lubrication theory. Although some results are reported, they are in isolation from the heat transfer and cure processes. The model proposed in [2] is, most likely, the first comprehensive model dealing with the curing of composites. Even so, the model treats separately the flow in the normal and parallel direction to the composite. In the normal direction the flow is assumed to behave as one-dimensional Darcy flow, and in the parallel direction, as a Poiseuille flow between parallel plates. In [2,3], it is assumed that the consolidation process is dominated by the resin flow. In [4], however, it is argued that the elastic fiber deformation is central to the process, and to its understanding. The reasoning, is that the applied pressure, resin pressure and pressure supported by the fibers, when multiplied by appropriate areas, should balance, if the inertial effects are negligible. The viscoelastic behavior of the fibers/resin system is represented by a parallel, nonlinear spring/damper set. In [5,6], the original concept presented in [4] is further refined, and supporting experiments prove its validity. A similar concept is presented in [7,8], where the consolidation mechanism follows a piston/spring analogy apparently borrowed from soil consolidation theory. In [7], it is demonstrated that for thick laminates most of the resin flow is along the laminate fiber bundles, i.e., the flow is parallel.

The study reported in [8] presents one of the first models, which couples the flows in different directions using the assumption of Darcy flow. This unified approach has the advantage of predicting a single pressure value for each location at each instant of time. The only shortcoming is the need for accurate models to predict the permeabilities, and in particular, the transverse permeabilities when dealing with thick laminates. The work described in [9] addresses this particular issue. The composite is assumed to be transversely isotropic, i.e., the two transverse permeabilities are the same. A semi-empirical Carman–Kozeny equation modified to fit the experimental data is proposed to predict the transverse permeabilities. The mathematical model proposed in [9], with different levels of simplifying assumptions, was used in the analyses appearing in [1,10–13], as will be discussed later on.

2.3. Thermo-kinetics

The work reported in [14] was critical in establishing the parameters to describe the resin kinetics and rheological behavior of Hercules ASA/3501-6 tape. The resin kinetics is based on a modified Arrhenius equation, and it allows the calculation of the resin conversion and consequent mass generation. The work of [15] corroborates the rheological model of [14], and optimized cure cycles are obtained by using the data of [14] and experimental tests. A comprehensive study of the thermal model for the cure of thermoset composites can be found in [16]. Similar models and experimental techniques to those in [14] are used in [17] to characterize other graphite/epoxy composites—Hexcel F584, and ACC 919.

3. Model

The governing equations describing the model selected—based on the literature survey and numerical tests conducted, are given in the following sections.

3.1. Flow model

The applied pressure, σ, is calculated using an equilibrium equation [7] relating it to the effective pressure sustained by the fibers, p_f, and the resin, p_r, namely:

$$\sigma = p_r + p_f \tag{1}$$

The assumption of Darcy flow for the resin, and the additional simplifications that the pemeabilities, S_{ij}, are equal to zero if $i \neq j$, yields:

$$m_v \frac{\partial p_r}{\partial t} = \frac{\partial}{\partial x}\left(\frac{S_{xx}}{\mu}\frac{\partial p_r}{\partial x}\right) + \frac{\partial}{\partial y}\left(\frac{S_{yy}}{\mu}\frac{\partial p_r}{\partial y}\right) + \frac{\partial}{\partial z}\left(\frac{S_{zz}}{\mu}\frac{\partial p_r}{\partial z}\right) \tag{2}$$

where $m_v = a_v/(1+e)$, $a_v = -\partial e/\partial p_f$, and $e = V_r'/V_f'$. V_r' is the volume of resin and V_f' is the volume of fibers. The value of a_v is determined based on the experimental data of [5], and the reformulation of the data fitting reported in [11], namely:

$$a_v = \begin{cases} -2.122 \times 10^{-5}\ \text{Pa}^{-1} & \text{for } p_f < 3588\ \text{Pa} \\ -0.0786/p_f\ \text{Pa}^{-1} & \text{for } p_f > 3588\ \text{Pa} \end{cases}$$

The z- and x-direction correspond to the direction opposite to the applied force, and the direction parallel to the fiber bundles, respectively. The permeabilities and the viscosity of the resin are formulated as reported by Table 1.

Eq. (2) is obtained using the assumption of Darcy flow when the principal directions of the fiber coincide with those of the ordinates—a configuration, which corresponds to that being studied. For the general case, however, additional terms do arise, and the components of the permeability tensor can be obtained from the principal permeabilities as described in [10].

3.2. Thermo-kinetics

The energy equation, taking into account convected heat transfer and heat conduction in the three directions, is:

$$\frac{\partial}{\partial t}(\rho c T) + \rho_r c_r\left[\frac{\partial}{\partial x}(uT) + \frac{\partial}{\partial y}(vT) + \frac{\partial}{\partial y}(wT)\right] = \frac{\partial}{\partial x}\left(k_{xx}\frac{\partial T}{\partial x}\right) + \frac{\partial}{\partial y}\left(k_{yy}\frac{\partial T}{\partial y}\right) + \frac{\partial}{\partial z}\left(k_{zz}\frac{\partial T}{\partial z}\right) + \dot{m}'''\frac{e}{1+e}\Delta H \tag{3}$$

where T is the temperature, and u, v, and w are the velocity components in the directions x, y, and z, respectively. The properties ρ, c, and k_{ii} $(i = x, y, z)$ are the combined density, specific heat and thermal conductivity of the resin and fibers, respectively. The same symbols with the subscript "r" refer to the resin only. Table 1 reports on the values and/or formulation of these properties. One particular point should be clarified in what concerns the equation to determine k_{yy} and k_{zz}. In the original reference, [18], and in other publications, e.g., [1], the proposed formulation of the equation gives erroneous results, when the factor B is negative. The correct formulation is presented in Table 1.

Eq. (3), similarly to Eq. (2), is only valid when the ordinate directions coincide with the principal directions

Table 1
Modeling properties and parameters (AS4/3501-6)

Permeabilities:
Normal permeability [9]
$S_{xx} = \frac{r_f^2}{4K_{xx}}\frac{(1-V_f)^3}{V_f^2}$
(Carman–Kozeny equation)
Transverse permeabilities [9]
$S_{yy} = S_{zz} = \frac{r_f^2}{4K_{zz}}\frac{[(V_a'/V_f)^{1/2}-1]^3}{V_a'/V_f+1}$
V_f = fiber volume fraction $(0.50 < V_f < 0.80)$
K_{xx} = Kozeny constant (0.7)
r_f = fiber radius (for AS-4 fibers $= 4 \times 10^{-6}$ m)
K_{zz} = model constant (0.2)
V_a' = volume fraction for which all flow is shut off $(0.76 < V_a' < 0.82)$, suggested value: 0.80

Parameters of resin kinetics [14]:
$A_1 = 2.101 \times 10^9\ \text{min}^{-1}$
$A_2 = -2.014 \times 10^9\ \text{min}^{-1}$
$A_3 = 1.960 \times 10^5\ \text{min}^{-1}$
$\Delta E_1 = 8.07 \times 10^4\ \text{J·mol}^{-1}$
$\Delta E_2 = 7.78 \times 10^4\ \text{J·mol}^{-1}$
$\Delta E_3 = 5.66 \times 10^4\ \text{J·mol}^{-1}$
$\Delta H = 473.6 \pm 5.4\ \text{kJ·kg}^{-1}$, suggested value: $474\ \text{kJ·kg}^{-1}$

Physical and thermal properties AS/3601-6 [2]:
Resin density: $1260\ \text{kg·m}^{-3}$
Specific heat of resin: $1.26\ \text{kJ·kg}^{-1}\text{·K}^{-1}$
Thermal conductivity of resin: $0.167\ \text{W·m}^{-1}\text{·K}^{-1}$
Initial prepeg resin mass fraction: 42%
Initial thickness of a prepeg: 1.651×10^{-4} m
Fiber density: $1790\ \text{kg·m}^{-3}$
Specific heat of fiber: $0.712\ \text{kJ·kg}^{-1}\text{·K}^{-1}$
Thermal conductivity of fiber: $26.0\ \text{W·m}^{-1}\text{·K}^{-1}$

Mochburg bleeder cloth:
Apparent permeability: $5.6 \times 10^{-11}\ \text{m}^2$
Porosity: 0.57

Rheological model [14]:
$\mu = \mu_\infty \exp(U/RT + K\alpha)$
$\mu_\infty = 7.93 \times 10^{-14}\ \text{Pa·s}$
$U = 9.08 \times 10^4\ \text{J·mol}^{-1}$
$K = 14.1$
$R = 8.314\ \text{J·K}^{-1}\text{·mol}^{-1}$
Rule of mixtures used for the specific heat and the density

Conductivity model: proposed in [18] with due corrections
$k_{xx} = V_f k_f + V_r k_r$
$k_{yy}/k_r = k_{zz}/k_r = 1 - 2\sqrt{V_f/\pi} + \frac{1}{B}\left[\pi - \frac{4}{\sqrt{1-C}}\tan^{-1}\frac{\sqrt{1-C}}{1+B\sqrt{V_f/\pi}}\right]$
$B = 2(k_r/k_f - 1)$; $C = B^2 V_f/\pi$
V_r = resin volume fraction $(= 1 - V_f)$

Laminate:
Width: 0.254 m (10 in)
Length: 0.305 m (12 in)

of the fiber. Otherwise, the six components of the thermal conductivity tensor must be considered.

ΔH is the heat of reaction per unit mass of resin, and $\dot{m}'''$ is the mass conversion rate, which is determined by the species equation,

$$\rho_r \frac{\partial \alpha}{\partial t} = \dot{m}''' \tag{4}$$

$$\frac{\partial \alpha}{\partial t} = \begin{cases} (K_1 + K_2\alpha)(1-\alpha)(0.47-\alpha) & \text{for } \alpha \leqslant 0.3 \\ K_3(1-\alpha) & \text{for } \alpha > 0.3 \end{cases} \tag{5}$$

The resin kinetics in what concerns the relation between $\dot{m}'''$ and α is described by the experimental relations of [14], as proposed by [1]:

$$K_i = \frac{1}{60} A_i \exp(-\Delta E_i / RT), \quad i = 1, 2, 3 \tag{6}$$

The integration of Eq. (4) is performed with an explicit scheme as proposed in [19].

4. Numerical algorithm

The governing equations are discretized using a control-volume finite element method, and the solution approach follows the scheme proposed in [20], where the pressure-velocity coupling is not required due to the assumption of Darcy flow. Extensive numerical tests were conducted to evaluate grid convergence and convergence criteria.

To assess the Darcy flow model, it was assumed that parameters S_{ij}, m_v, σ, μ and the laminate thickness were constant during the consolidation process. This assumption implies the flow is independent of the thermal cycle, and the aim is use the analytical closed solution provided in [7]. Fig. 2 depicts the comparison between the present numerical results and those obtained using the closed solution of [7] for a $0.1524 \times 0.1524 \times 0.03556$ m^3, laminate under the following conditions: $\sigma = 689.4$ kPa, $m_v = 8.7025 \times 10^{-7}$ Pa^{-1}, $\mu = 10$ Pa·s, $S_{xx} = 6.45 \times 10^{-12}$ m^2, and $S_{yy} = S_{zz} = 6.45 \times 10^{-13}$ m^2. The analytical and numerical results shown are in clear agreement, which guarantees the accuracy of the flow model and its solution algorithm.

5. Results and discussion

The literature is scarce in what concerns three-dimensional modelling of the cure simulation of thick laminates, and in particular for situations, where resin flow may be a dominant process factor. One of the few attempts of three-dimensional modelling is reported in [11] for the thermal cycle depicted in Fig. 3, and for a composite AS4/3501-6 with 100 plies. The applied pressure is taken as 1.379 MPa to allow a comparison with the results of [1]. The edges of the laminate are not covered with the bleeder cloth, which yields a zero pressure drop. At the interface between the laminate and the metal tool is assumed the occurrence of no-flow. This

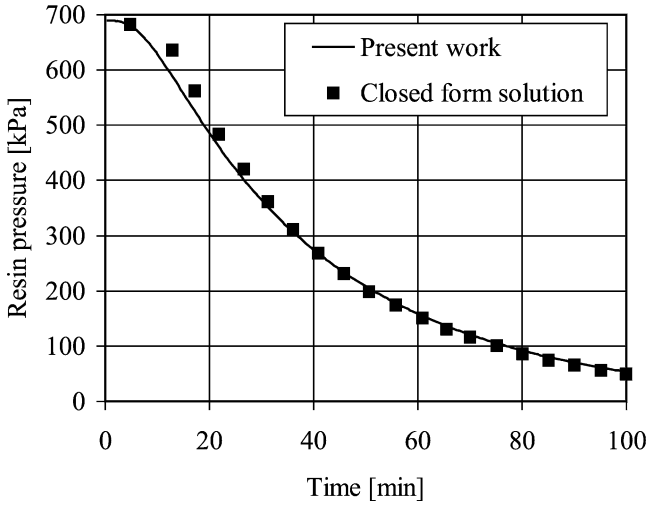

Fig. 2. Temporal development of the resin pressure at the center of the laminate: comparison between the obtained numerical results and the closed form solution.

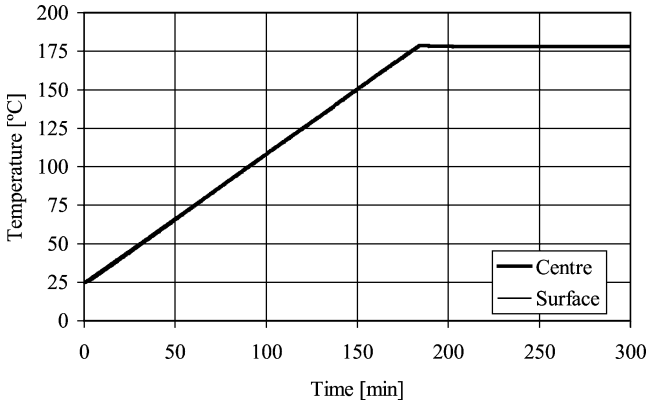

Fig. 3. Thermal profile for a 100-ply AS4/3501-6 with 1.379 MPa consolidation pressure.

condition in the algorithm is set by making at the interface $\partial p_r / \partial z = 0$.

To avoid further uncertainties with the thermal resistances associated with the bagging materials, the thermal cycle is directly imposed upon the surface of the laminate. This assumption also implies the occurrence of high recirculation flow within the autoclave.

The overall agreement between the present prediction and those of [1,10,11] is good for most parameters, however, the thickness reduction presents a few discrepancies, which deserve further attention.

Fig. 4 reports on the predictions obtained in the present work and those reported in [11], and it is apparent that they are in agreement up to approximately 90 minutes. Beyond this time instant, they diverge significantly. This was thought that it could be attributed to different constants used by [11] in the calculation of the transverse permeabilities. The use of these values, in the present model, however, did not bring any significant changes to the previous predictions.

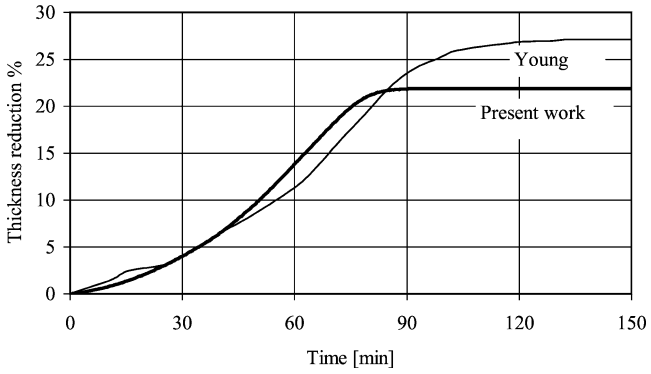

Fig. 4. Comparison between the present predictions and those of [11] for a 100-ply laminate with an applied consolidation pressure of 1.379 MPa, and a zero-bleeder pressure.

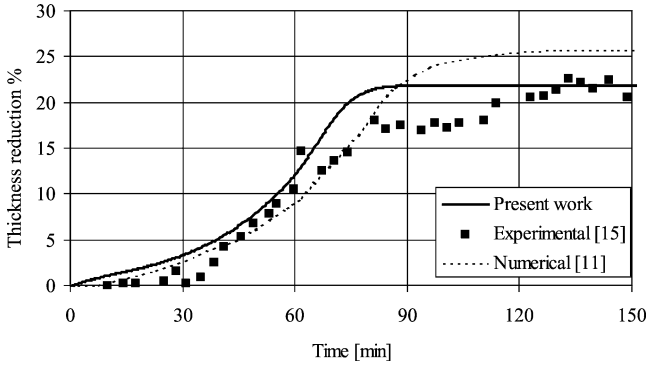

Fig. 5. Comparison of the present predictions and those of [11] against experimental data of [15] for a 52 ply laminate with an applied consolidation pressure of 1.379 MPa, and a bleed pressure of 0 MPa.

In an attempt to further evaluate the present model, present predictions and those of [11] were compared with the experimental data for a 52-ply laminate [15], as shown in Fig. 5. The comparison is not conclusive, but it seems that the present predictions yield values that better emulate the experimental data.

The prediction capability of the model is tested for a 400-ply laminate with a consolidation pressure of 2.07 MPa, and an arbitrary bleeder pressure of 0.5 MPa, which was specified by taking a prescribed pressure drop across the bleeder. The bleeder permeability is not used in the computation because the bleeder itself is not part of the simulation domain. The fibres are aligned along the larger of the two planar dimensions (0.305 m), and for the thermal cycle depicted in Fig. 6.

The temperature development with time at the center of the laminate is also shown in Fig. 6, and it is in good agreement (within 2% to 7%) with [1]. It is interesting to note at the center a slight temperature overshoot around 250 minutes, however the viscosity keeps increasing due to the high level of cure, as it can be noted in Fig. 7.

The interplay between temperature and degree of cure is well illustrated through the viscosity behavior. By "zooming" Fig. 7 in the region of 0 to 100 minutes, as shown in Fig. 8, it can be clearly noted the "downward-upward" trend,

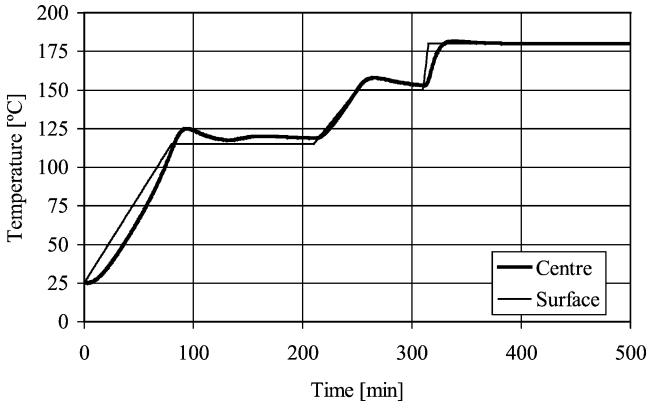

Fig. 6. Thermal cycle at the surface of a 400-ply AS4/3501-6 laminate with a consolidation pressure of 2.07 MPa, and bleeder pressure of 0.5 MPa, and temperature development with time at the centre of the laminate.

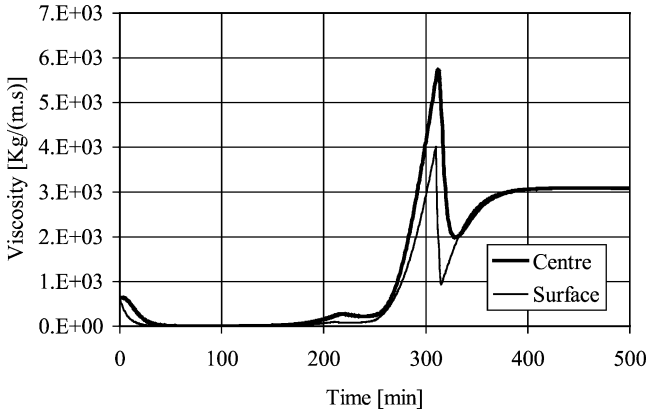

Fig. 7. Viscosity time history for the conditions reported for Fig. 6.

which corresponds to the dominance of the temperature first, and then that of the degree of cure.

The degree of cure at the surface and at the center, respectively, can be described by the resin conversion, α, as a function of time, as presented in Fig. 9.

The values of the pressure for the resin and the fibers, normalized with the consolidation pressure, are presented in Fig. 10, the corresponding conditions are those specified in Table 2.

Around 60–80 minutes, a drop in resin pressure occurs, and then the normalized value decreases to the corresponding asymptotic value. The percentual reduction in thickness of the laminate reaches its maximum reduction around 150 minutes, as shown in Fig. 11. It is interesting to see the effect of the bleed pressure upon the resin pressure, and for that matter, upon the fibre pressure. The normalized resin pressure, for instance, is much higher for case A than for case B, a result that might be expected. The results should be analyzed in light of the relation between the laminate permeability and the fiber volume fraction. The laminate permeability decreases always during the consolidation process due to the fiber volume fraction increase. Therefore, an increase of the resin pressure at the edges due to the presence of the bleeder (cases A and C) should provide a lower fiber

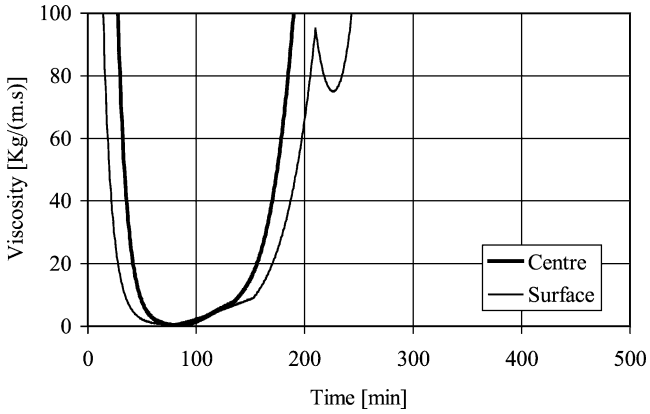

Fig. 8. Detail of the viscosity profile.

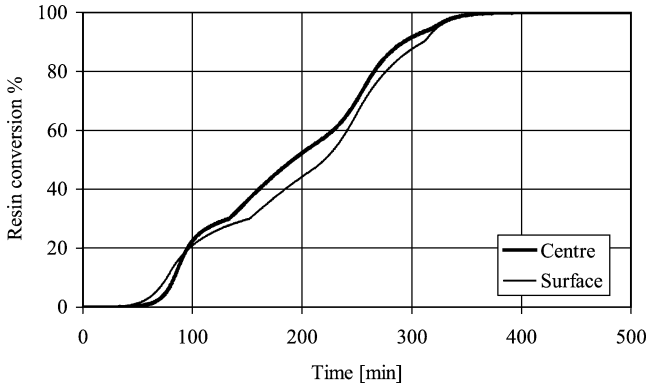

Fig. 9. Resin conversion, α, as a function of time.

Table 2
Conditions for the cases analyzed

Case	Plies	σ [Mpa]	P_{bleeder} [MPa]
A	400	2.07	0.5
B	400	2.07	0.0
C	100	2.07	0.5

volume fraction at the edges, thus promoting the resin outflow through the edges. In case B, a zero resin pressure at the edges leads to a greater fiber volume fraction and to a lower permeability, thus yielding a stronger resistance for the resin outflow through the edges.

For completeness and comparison purposes, Fig. 11 presents the three cases A, B and C, just discussed. Case C, as expected (100 plies vs 400 plies), is the one, out of the three cases, presenting the highest thickness reduction.

The resin final pressure distribution for case B, within the laminate, can be visualized through the isobars depicted in Fig. 12.

It should be mentioned that many parametric tests were conducted to evaluate the relative importance of the advection terms in the energy equation. It was found that only in a narrow time "window" (0 to ∼100 minutes) they attain a magnitude close to the diffusion terms, then their relative value drops rapidly. This justifies their non-inclusion in the

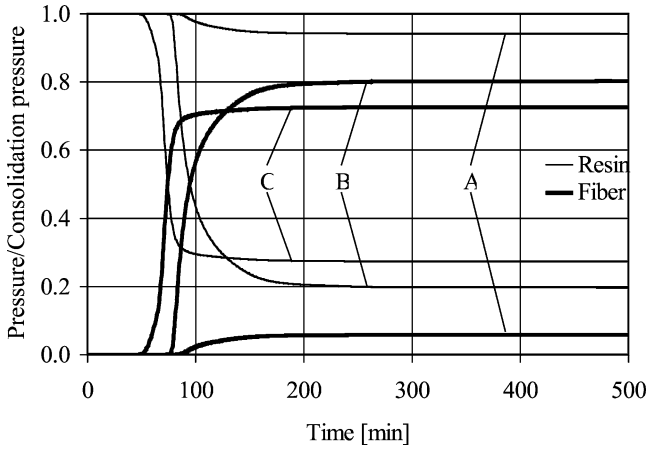

Fig. 10. Normalized pressure for resin and fibers at the center of the laminate for different conditions.

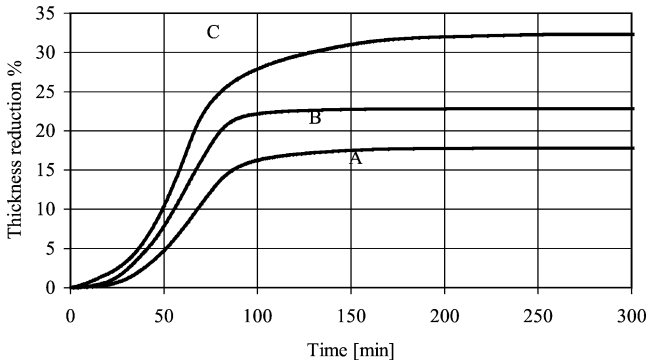

Fig. 11. Percentual reduction of the laminate thickness with time for different conditions.

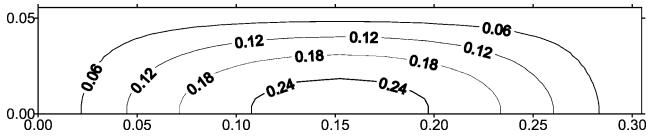

Fig. 12. Normalized pressure for resin (at the center of the laminate) at the end of the cure for case B.

formulation of the energy equation, which is the formulation path followed by many authors, e.g., [19].

6. Concluding remarks

The numerical model proposed is the result of an extensive testing and evaluation, and to a great extent, is a "state-of-the-art" tool for the thermal analysis of epoxy/graphite based composites obtained through the cure in autoclave. The results seem to emulate well the physical phenomena, and they are in good agreement with data reported in the open literature. The results clearly identify a temperature overshoot in the center of the laminate composite during the curing process. This phenomenon was observed by other authors, and it is important in what concerns the eventual void formation and its effect upon the integrity and quality of

the final product. The model also describes well the role of the bleeder, i.e., its presence yields an increase of the resin pressure at the edges, which, in turn, locally decreases the fiber volume fraction facilitating the resin outflow through the edges. The available literature seems to have neglected to report on how the bleeder pressure influences the permeability and fiber volume fraction through the resin pressure.

Acknowledgement

The support received by the project through the NSERC (Canada) Individual Innovation Grant (ACMS), OGP0001398, and from the "Mechanical Technology and Automation" R&D Unit (University of Aveiro) are gratefully acknowledged.

References

[1] W.B. Young, Compacting pressure and cure cycle for processing of thick composite laminates, Compos. Sci. Technol. 54 (1995) 299–306.
[2] A.C. Loos, G.S. Springer, Curing of epoxy matrix composites, J. Compos. Materials 17 (1983) 135–169.
[3] J.T. Lindt, Engineering principles of the formation of epoxy resin composites—Mathematical model of the fluid flow, SAMPE Quarterly 5 (1982) 14–19.
[4] T.G. Gutowski, A resin flow/fiber deformation model for composites, SAMPE Quarterly 6 (1985) 58–64.
[5] T.G. Gutowski, Z. Cai, J. Kingery, S.J. Wineman, Resin flow/fiber deformation experiments, SAMPE Quarterly 27 (4) (1986) 54–58.
[6] T.G. Gutowski, T. Morigaki, Z. Cai, The consolidation of laminate composites, J. Compos. Materials 21 (1987) 172–188.
[7] R. Dave, J.L. Kardos, M.P. Dudukovic, A model for resin flow during composite processing: Part I—General mathematical development, Polym. Compos. 8 (1987) 29–38.
[8] R. Dave, J.L. Kardos, M.P. Dudukovic, A model for resin flow during composite processing: Part II—Numerical analysis for unidirectional graphite/epoxy laminates, Polym. Compos. 8 (1987) 123–132.
[9] T.G. Gutowski, Z. Cai, S. Bauer, D. Boucher, J. Kingery, S. Wineman, Consolidation experiments for laminate composites, J. Compos. Materials 21 (1987) 650–669.
[10] W.B. Young, Resin flow analysis in the consolidation of multi-direction laminated composites, Polym. Compos. 16 (1995) 250–257.
[11] W.B. Young, Consolidation and cure simulations for laminated composites, Polym. Compos. 17 (1996) 142–148.
[12] P. Hubert, Aspects of flow and compaction of laminated composite shapes during cure. Ph.D. Thesis, University of British Columbia Vancouver, BC, 1996.
[13] D.C. Blest, B.R. Duffy, S. McKee, A.K. Zulkifle, Curing simulation of thermoset composites, Composites: Part A 30 (1999) 1289–1309.
[14] W.J. Lee, A.C. Loos, G.S. Springer, Heat of reaction degree of cure and viscosity of Hercules 3501-6 resin, J. Compos. Materials 16 (1982) 510–520.
[15] P.R. Criscioli, Q. Wang, G.S. Springer, Autoclave curing—Comparisons of model and test results, J. Compos. Materials 26 (1992) 90–102.
[16] S.P. Kinsey, A. Haji-Sheikh, D.Y.S. Lou, A thermal model for cure of thermoset composites, J. Mat. Process. Technol. 63 (1997) 442–449.
[17] D. Frank-Susich, D.H. Laananen, D. Ruffner, Cure cycle simulation for thermoset composites, Compos. Manufacturing 4 (3) (1993) 139–146.
[18] G.S. Springer, S.W. Tsai, Thermal conductivities of unidirectional materials, J. Compos. Materials 1 (1967) 166–173.
[19] S.C. Joshi, X.L. Liu, Y.C. Lau, A numerical approach to the modeling of polymer curing in fibre-reinforced composites, Compos. Sci. Technol. 59 (1999) 1003–1013.
[20] V.A.F. Costa, L.A. Oliveira, A.R. Figueiredo, A control-volume based finite element method for three-dimensional incompressible turbulent fluid flow, heat transfer, and related phenomena, Internat. J. Numer. Meth. Fluids 21 (1995) 591–613.